Colloid Polym Sci 273: 633–641 (1995)

ORIGINAL CONTRIBUTION

Y. Sugiura
Y. Makimura
Y. Kita
M. Matsuo

Morphology and mechanical properties of ultra-high molecular weight polyethylene-poly(tetrafluoroethylene) blend films

Received: 22 August 1994
Accepted: 24 January 1995

Y. Sugiura · Dr. M. Matsuo (✉)
Department of Textile and Apparel Science
Nara Women's University
Nara 630, Japan

Y. Makimura
Takiron Co. Ltd.
Ibogun Hyogo 671 - 13, Japan

Dr. Y. Kita
Osaka Municipal Technical Research Institute
Osaka 536, Japan

Abstract This paper deals with the morphology and mechanical properties of blend films for polytetrafluoroethylene (PTFE) and ultra-high molecular weight polyethylene (UHMWPE) prepared by kneading techniques. This experiment was carried out for blend films, prepared with different compositions of PTFE and UHMWPE to improve thermal properties of PE. In spite of the incompatibility of the two polymers, the blend film with the PTFE/UHMWPE composition = 75/25 was maintained under the measurement of complex modulus at temperature higher than 300 °C. This indicates that the UHMWPE chains dispersed in PTFE fibrous texture were not separated by the melting flow of UHMWPE at 300 °C. To check the origin of this interesting phenomenon, the morphology of the blend films was investigated by using scanning electron microscopy, X-ray diffraction, and ^{13}C nuclear magnetic resonance.

Key words Blend films – polytetrafluoroethylene – ultra-high molecular weight polyethylene – thermal properties – morphology

Introduction

Since 1974, the preparation of polymeric fibers and films with high strength and high modulus has been extensively investigated for ultra-high-molecular-weight-polyethylene (UHMWPE) with viscosity-average molecular weight of 2 million, by gel-state spinning [1], ultradrawing of dried gel films [2–5] and ultradrawing of single crystal mats [6, 7]. For specimens with draw ratio higher than 200, the Young's modulus reached more than 200 GPa and the value was nearly equal to the crystal lattice modulus (225–235 GPa) as measured by x-ray diffraction [8]. In comparison with traditional metals, the range of application of high modulus and high strength polyethylene is limited because of its low melting point. To improve the heat-resistance, crosslinking of amorphous chains has been performed by γ- and electron beam irradiation [9, 11] and chemical reaction [12, 13]. The Young's modulus decreased drastically at temperature > 150 °C, although the cross-linked specimen by chemical reaction was not melted even at temperatures > 200 °C. This is due to the melting of crystallites, independent of cross-linking [3].

To avoid the drastic decrease of the Young's modulus around the melting point, the blend gel films of UHMWPE and ultra-high molecular weight polypropylene (UHMWPP) were prepared with different components [14, 15]. The specimens were certainly maintained without drastic decrease of the Young's modulus when the content of UHMWPP of blend films was higher than 50% [15]. The specimen was melted at around 180 °C, close to the melting point of PP. These results indicate that one of the important factors to improve the heat resistance of PE is due to the preparation of blend films of PE and other polymer having no flowability. For this purpose, several

trails have been done by using polytetrafluoroethylene (PTFE) with very stable thermal properties and no thermal flowing [16, 17].

The blend of high-density polyethylene (HDPE)-PTFE was made by Nagarajan et al. [7]. They studied the morphology by infrared red, nuclear magnetic resonance, and ESCA measurements in terms of molecular interaction between two constituent phases. They suggested that the interdiffusion of PE and PTFE chains occurs at the interface and results in the transitional layers. They pointed out that the presence of such a transitional layer may be responsible for the deviation of absorbance and the second moment from the law of simple mixture.

Based on their concept, this paper deals with the preparation of UHMWPE-PTFE blend films by kneading techniques to promote the heat-resistance of PE. The difficult problem in preparing the blend films is due to the fact that the degradation has not been avoided under the kneading process. In this consideration, UHMWPE was used in the present work in order to avoid the decrease in molecular weight as much as possible. The UHMWPE and PTFE powders were kneaded at high temperatures $> 300\,^{\circ}C$ under nitrogen. The morphology and mechanical properties of the resultant films were checked by scanning electron microscopy, x-ray diffraction, ^{13}C NMR and dynamic tensile modulus.

Experimental section

Sample preparation

A linear polyethylene (Hercules 1900/90189) with an intrinsic viscosity of 30 dl/g, corresponding to a molecular weight of 6×10^6 was used as a specimen. Polyfron M-12, was used as a test specimen of PTFE, which was obtained from Daikin Eng. Co. Ltd. The PTFE/UHMWPE compositions chosen were 100/0, 75/25, 50/50, 25/75, and 0/100 by weight.

The torque-rheometer, Haake Rheocord 90, was employed to knead the PTFE and UHMWPE powder. The mixing was done by rotating at 60 r.p.m. at an initial temperature of 320 °C for 5 min under nitrogen flow. The actual temperature in the torque rheometer deviated from the initial temperature and the behavior is shown in Fig. 1. The temperature decreased at the initial stage and then increased. Through several repeated measurements, this tendency was found to be similar for all the compositions. This is thought to be due to the frictional condition between blend powder and/or fluid and the torque. All mixtures were cooled down immediately to room temperature and then pressed at 320 °C under 19.6 MPa for 5 min. Incidentally, the drastic degradation of molecular weight

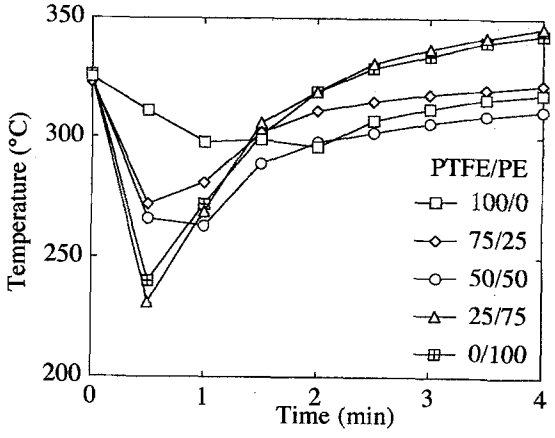

Fig. 1 Time dependence of temperature in the torque-rheometer

of UHMWPE was confirmed by using the homopolymer from viscosity measurements and this is due to the heat-inferiority during the kneading at 320 °C in the torque-rheometer. That is, at 0.1 g/100 ml concentrations, the reduced viscosity decreased from 53.8 dl/g to 2.5–8 dl/g by the heat treatment for 5 min in the torque rheometer at 320 °C.

Sample characterization

The thermal behavior was estimated from the endothermic peaks in differential scanning calorimetry (DSC) curves. Specimens, weighing about 10 mg, were placed in a standard aluminum sample pan. Samples were heated at a constant rate of $10\,^{\circ}C\,min^{-1}$. To estimate the crystallinities of UHMWPE and PTFE within the blend films, the heat of fusion was estimated on the basis of the value of metallic references such as Pb, In, and Sn.

The complex dynamic tensile modulus function was measured at a frequency of 10 Hz over the temperature range from $-100°$ to 300 °C. The length of the specimen between the jaw was about 40 mm and the width was 2 mm. The specimen was heated at a constant rate of $2\,^{\circ}C\,min^{-1}$. During measurements, the specimen was subjected to a static tensile strain in order to place the specimen in tension during the axial sinusoidal oscillation to assure viscoelastic behavior of the specimen. The static strain was set at a suitable value at each temperature and the value tended to increase slightly with temperature in the range from 0.02 to 2%.

The x-ray measurements were carried out with a 12-kW rotating-anode x-ray generator (Rigaku RDA-rA) [14]. The x-ray beam was monochromatized with a curved graphite monochrometor using CuK_α radiating at 200 mA

and 40 kV. The wide-angle x-ray diffraction (WAXD) patterns were obtained with a flat camera. WAXD intensity distribution was measured by point focus at a step interval of 0.1° with a time interval of 40 s, in the desired range of twice the Bragg angle. The diffraction beam was detected by a square slit of 1 mm × 1 mm.

^{1}H DD/MAS ^{13}C NMR measurements were carried out at room temperature with a JEOL-JM-EX270 spectrometer operating at a field of 6.35 T. The radio frequency of 67.5 MHz was used for detection of ^{13}C resonance. MAS was carried out at a rate of 4.5 kHz with a cylinder-type rotor made of zirconia/polyimide. The chemical shifts relative to tetramethylsilane (Me_4Si) were determined from the CH line (29.5 ppm) of solid adamantane as an external resonance.

The pulse sequences used are schematically shown in Fig. 2. Pulse sequence (a) with cross-polarization (CP) developed by Torchia [18] was used to measure the spin-lattice relaxation time, which was used to measure T_{1c} values longer than several tens of second. The spin-lattice relaxation time shorter than a few seconds was measured by standard saturation-recovery pulse sequence (b) without CP. Pulse sequence (c) was used to estimate ^{13}C spin-relaxing of the transverse magnetization without 1 H decoupling for a given time interval τ. It is possible to estimate the contribution from a rapid or less mobile component by a proper choice of τ.

Fig. 2 The pulse sequence (a) cross-polarization by Torchia, (b) the standard saturation-recovery pulse sequence, (c) transverse magnification

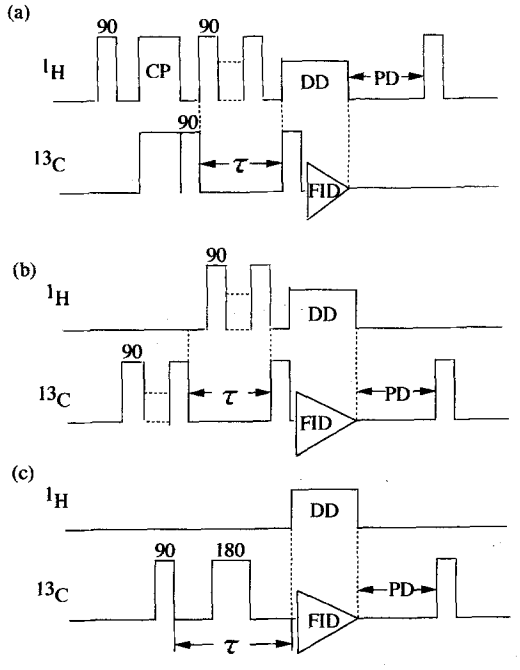

Scanning electron micrographs were obtained with a JSM-T300. Because of flat surface of pressed films, the PFTE/UMWPE blend films were immersed in decalin at 140 °C for 1 h to remove UHMWPE. Thus, the observation was made for fibrous textures of the residual PTFE.

Results and discussion

Figure 3 shows the change in the profile of the DSC curves with different PTFE/UHMWPE compositions. To check the reproducibility of the profile, DSC measurements of a given composition were carried out several times. It is seen that the DSC curves exhibit separate endotherms corresponding to the individual homopolymers. The peak at lower temperature is due to UHMWPE and the other is due to PTFE. The melting point of UHMWPE was almost independent of the composition, while the melting point of PTFE slightly decreased with increasing the content of UHMWPE. Close observation reveals that the DSC curves for the blended films and the UHMWPE homopolymer film show a very dull peak associated with exotherm phenomenon in the range 180°–250 °C, but such a peak has never been observed for the PTFE homopolymer film. The peak shifts to higher temperature with increasing of the PTFE content. The appearance of the peak is probably due to the carbonization, since the specimens prepared by the kneading at 320 °C showed light yellow.

To check the crystallinity of each component within the blend films, the values, 68.5 cal/g [19] and 22.2 cal/g [20] were employed as the heat of fusions of PE and PTFE at 100% crystallinity, respectively. Fig. 4 shows the results.

Fig. 3 The profile of DSC curves measured for the blend films with different compositions

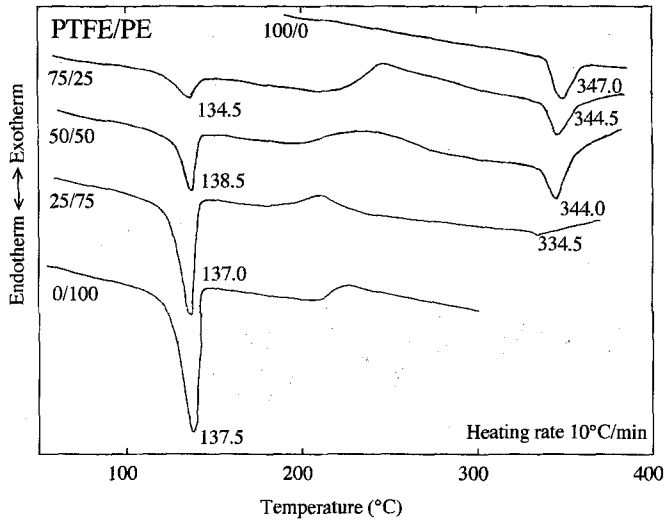

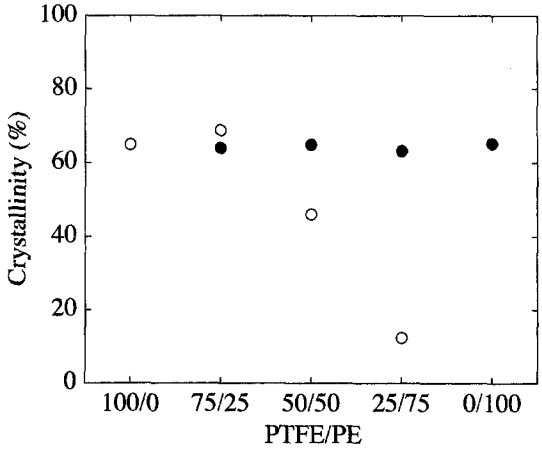

Fig. 4 Crystallinity of PTFE and PE within the blend films estimated by heat of fusions

The crystallinities of UHMWPE were in the range 61–62.5%, which is almost independent of the composition. In contrast, the crystallinity of PTFE decreased drastically with increasing of the UHMWPE content. Especially, the crystallinity of the film with 25/75 composition was shown to decrease to less than 20%.

To check the heat-resistance effect as a function of the component, the temperature dependence of the complex dynamic tensile modulus was observed. Fig. 5 shows the results. It should be noted that the specimens with the 50/50 and 75/25 compositions could be maintained around up to 200° and above 300 °C, respectively, reflecting the heat-resistance effect of PTFE higher than 300 °C. This indicates that the increase in PTFE content plays an important role to improve the heat-resistance effect. The storage modulus E' of PTFE decreases around 20 °C and tends to decrease gradually. The loss modulus E'' shows a peak around 20 °C corresponding to the decrease of E'. The mechanical dispersion around 20 °C has been known as the β dispersion associated with the crystal transition at room temperature. However, the α and γ dispersions associated with the amorphous region for PTFE homopolymer has never been observed clearly [21], although they are reported to have peaks around $-100°$ and 125 °C, respectively. This is thought to be probably due to high crystallinity.

The value of E' for UHMWPE has one peak around 80 °C associated with the crystal dispersion (the α dispersion) which has been usually reported to be classified into two mechanism, the α_1 and α_2 mechanisms [22, 23]. The β dispersion associated with the amorphous region was not observed clearly, but it did occur around -20 °C for melt films. The temperature dependence of E' and E'' for the blend films is affected by that of each homopolymer.

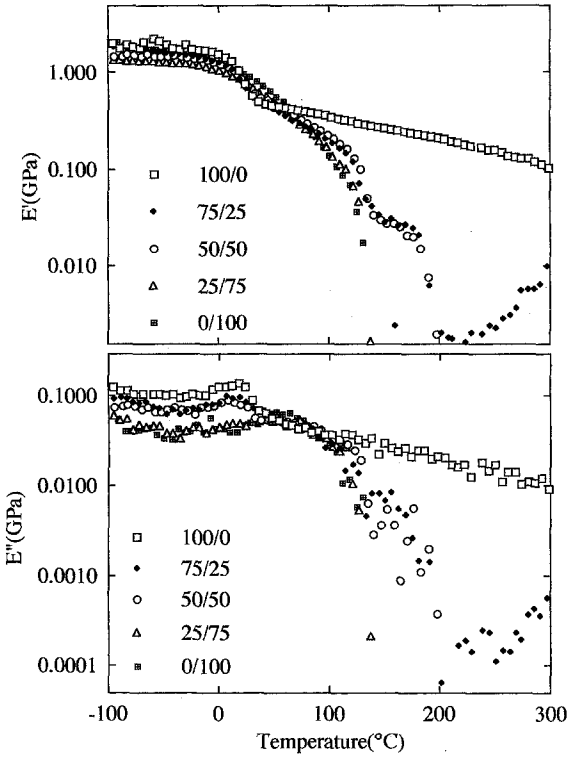

Fig. 5 Temperature dependence of the complex dynamic tensile modulus for the blend films

That is, for the blended films with the 75/25 and 50/50 compositions, the β dispersion can be observed clearly, while for the 25/75 composition, the appearance of the α dispersion became distinct. This indicates that the temperature dependence of the storage and loss moduli of the blended films is slightly sensitive to the content of two homopolymers on the basis of the composite law of mechanical properties. However, only abnormal behavior can be observed for the 75/25 blended film at temperature > 200 °C. In that temperature range, the storage and loss moduli increased with temperature, indicating rubber elasticity of UHMWPE. If this is the case, it may be expected that the two homopolymers become intimately mixed in spite of their compatibility.

Figure 6 shows WAXD patterns for the 75/25 blend film as a function of temperature. The clear ring belongs to the reflection from the (100) plane (or the (010) plane) of PTFE [24]. The reflections from the (110) and (200) planes of PE are very weak because of the 25% content, which are observed as indistinct rings outside the (100) reflections of PTFE. The two weak reflections were maintained at 140 °C. The reflections disappeared due to melting at 180 °C and appeared again at 27 °C with recrystallization of PE chains.

Returning to Fig. 5, it is seen that the storage modulus increased with temperature higher than 200 °C due to

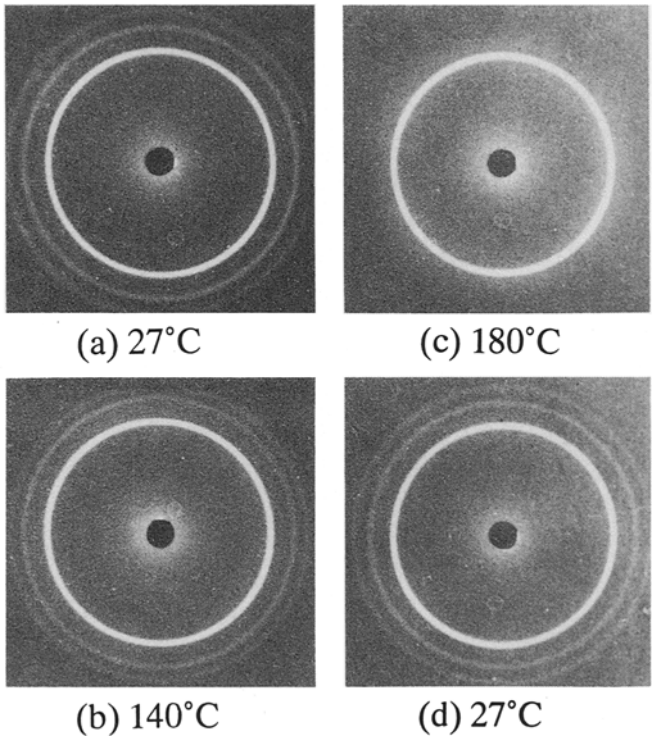

Fig. 6 WAXD patterns for the 75/25 blend film as a function of temperature

rubber elasticity of PE chains within the film with the 75/25 composition. This indicates the PE chains dispersed in PTFE matrix were not free to allow flow at temperature above the melting point of PE because of no flow of PTFE chains. If PE chains were not connected with PTFE matrix, PE chains took random coils and then any increase in the storage modulus in the temperature range $> 200\,°C$ could not be observed.

In order to facilitate understanding the concept, the observations were done under scanning electron microscopy using the residual films obtained after removing UHMWPE by immersing the blend films into decalin solvent for 1 h at 140 °C. The photographs on the left-hand side of Fig. 7 show the change in appearance of the residual PTFE under scanning electron microscopy, in which PTFE/UHMWPE composition reveals the component of the original blend film before removing UHMWPE and those on the right-hand side, that magnified. As illustrated in the six micrographs, observation reveals that the fibrillar texture is sponge-like. Judging from the heat-resistance of the original films with the 75/25 and 50/50 compositions shown in Fig. 5, UHMWPE chains within PTFE matrix are evidently not free to allow flow at the melt state. Accordingly, it may be expected that UHMWPE chains diffused within the PTFE fibrillar textures under the kneading process could not be separated from PTFE matrix. This is probably attributed to the long length of UHMWPE chains. Actually, we confirmed that the spectrum of infra red exhibited the very small residual traces of UHMWPE within the specimens.

Figure 8 shows WAXD intensity distribution for the blend films to check the mechanism of crystal growth for all the compositions. The measurements were carried out as a function of $2\theta_B$ and corrections were made for air scattering, polarization and absorption. But, the incoherent scattering was neglected because of the complicated treatment for the blended system. As illustrated in the five diagrams, the content of UHMWPE causes significant effect on the crystallization of PTFE. In diagrams (a) and (b), it is seen that the diffraction intensity from the (100) plane (or (010) plane) of PTFE is proportional to the content of PTFE and is hardly affected by the introduction of the UHMWPE, while the intensities from the (106) and (107) planes decrease drastically. This means that the crystal growth in the lateral direction is hardly affected by the increase in the UHMWPE content, while the growth of crystallites in the chain direction hampers by the introduction of UHMWPE and this effect is obviously related to the decrease of crystallinity shown in Fig. 3. As for the UHMWPE, the diffraction from the (002) plane was too weak even for a homopolymer film to detect the influence of the content of PTFE. Here, it should be noted that the poor growth of PTFE crystallite in the chain direction indicates the large occupation of amorphous region in a chain. If the amorphous chain segments of PTFE cause significant mobility under shear stress occurring because of kneading at 320 °C, in spite of no thermal flow of PTFE, the possibility of entanglements between UHWPE and PTFE chains may be expected. However, this remains an unresolved problem.

The change in crystal sizes for the blend system must be estimated as a function of the composition by using Scherrer's equation from the integrated breadth. In doing so, we have tried to subtract the contribution of amorphous phase from the intensity distribution in Fig. 8. Unfortunately, this trial was impossible for the blend system, since the profiles of the total amorphous regions of the PTFE and UHMWPE could not be determined because of the complicated overlapping of the diffraction peaks. Only rough estimation was done in the region of twice the Bragg angle $< 30°$, because of the simple profiles of intrinsic diffraction intensity peaks from PTFE and UHMWPE crystals. The estimation for each isolated peak was done using the modified intensity associated with the intensity distribution from an ideal pin hole. This method is described in the Appendix.

Table 1 shows the crystal size of PTFE and UHMWPE. The crystal size of PTFE crystallites perpendicular to the chain direction is almost independent of the

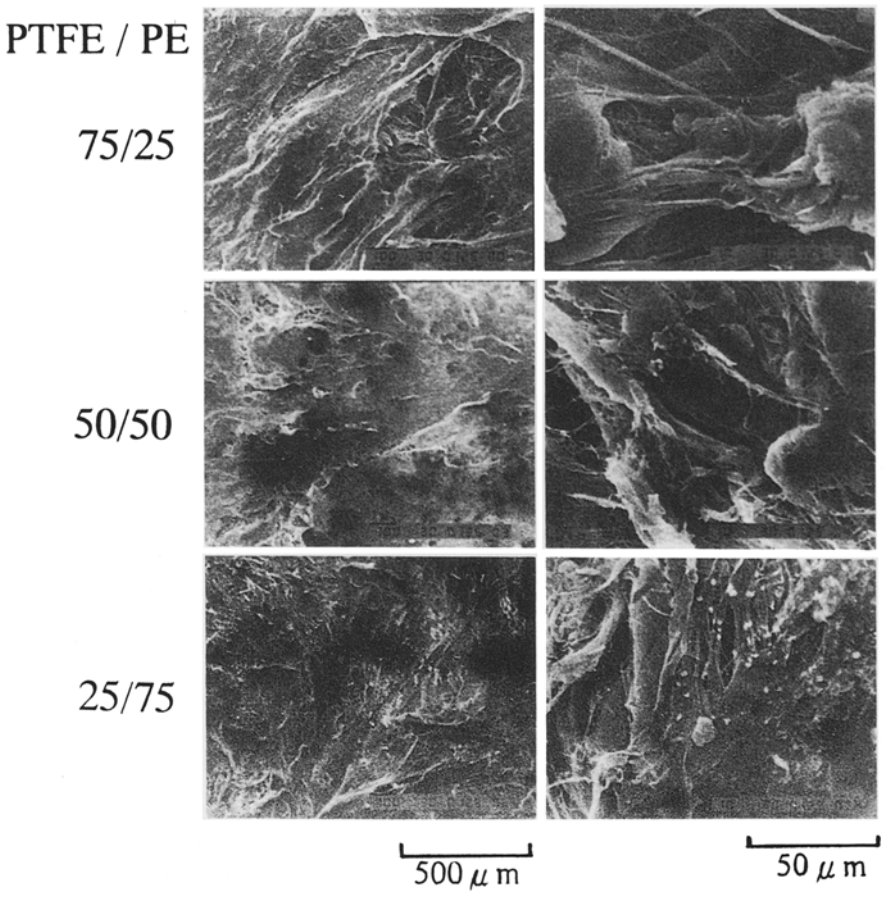

Fig. 7 Scanning electron micrographs of the 75/25, 50/50, and 25/75 compositions

composition. As for UHMWPE, the size is also independent of the composition, but is smaller than that of the homopolymer. This indicates that the growth of UHMWPE crystallites is slightly suppressed by the introduction of PTFE.

To facilitate understanding of the characteristics of crystalline and noncrystalline regions of UHMWPE by the introduction of PTFE, T_{1c} and T_{2c} were measured by pulse sequence (a) in Fig. 2 developed by Torchia [18] or by the standard saturation-recovery pulse sequence of (b). In doing so, the total magnetizations $M_c(\tau)$ were classified to reveal components as follows:

for Torchia's pulse sequence

$$M_c(\tau) = 2\sum_{i=1}^{N} M_{c,i}\exp(-\tau/T_{1c,i}), \quad (1)$$

and for the standard recovery pulse sequence

$$M_c(\tau) = \sum_{i=1}^{N} M_{c,i}(\infty)\{1-\exp(-\tau/T_{1c,i})\}, \quad (2)$$

where $M_{cp,i}$ is the ^{13}C magnetization of the i-th component after CP and $M_{c,i}(\infty)$ is the equilibrium ^{13}C

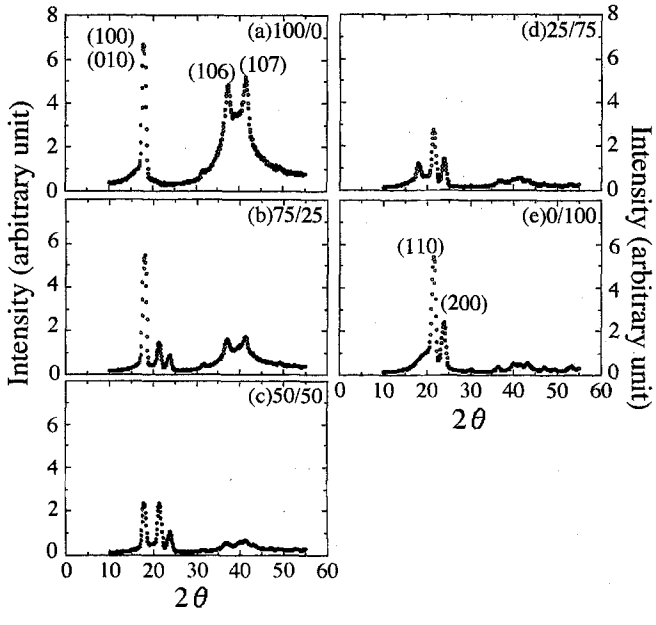

Fig. 8 WAXD intensity distribution for the blend films with the different PTFE/UHMWPE compositions: (a) 100/0, (b) 75/25, (c) 50/50, (d) 25/75, and (e) 0/100

Table 1 Crystal size of PTFE and PE within the blend films estimated by x-ray diffraction. unit (Å)

Sample (PTFE/UHMWPE)	PTFE (100) (010)	PE (110)	(200)
100/0	85–90	–	–
75/25	85–90	85–91	91–97
50/50	85–90	80–86	90–94
25/75	79–85	80–86	91–96
0/100	–	101–107	97–103

magnification of the i-th component. To satisfy Eq. (1), ^1H magnification must be zero or of constant value. For this purpose, the interval t was set to reveal 100 ms to satisfy the relationship $T_{2H} < t < T_{1H}$, since it must be saturated by $^1H90°$ multiple pulses given at t in the range 10–20 ms [25]. The value is variable for each specimen. The value of PD was chosen to be longer than five times the longest T_{1H} for each specimen.

Figure 9 shows the semilogarithmic plot as a function of τ for the ^{13}C magnetization of the peak height of the line at 33 ppm associated with the orthorhombic crystal form

Fig. 9 Semilogarithmic plot as a function of τ measured for the blend film with the 25/75 composition to measure T_{1c}. (a) an overall decay curve, (b) a middle slow decay curve, (c) a rapid decay curve

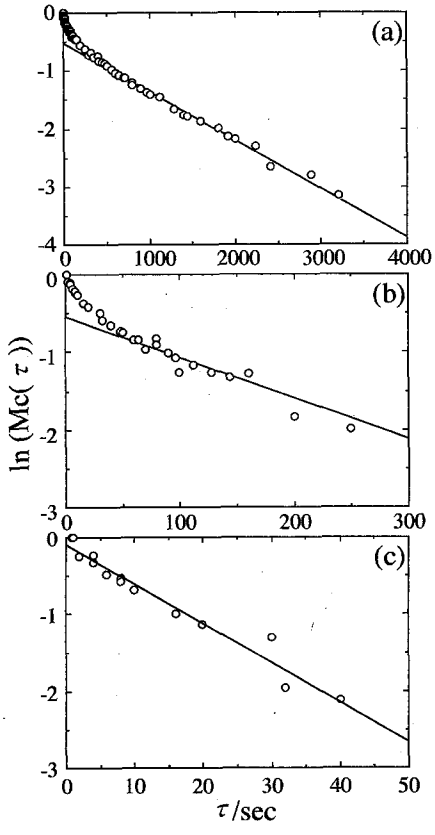

corresponding to the average of the principal values of the chemical shift tensor for trans-trans methylene sequence [26–28] measured for the 25/75 composition. Except UHMWPE, the overall decay curve (a) can be classified into three components by using a least square method with a computer; a slow decay curve (a), a middle slow decay curve (b), and a rapid decay curve (c) [25–29]. However, the middle slow decay curve for UHMWPE homopolymer was further classified into two components to obtain the best fit of the overall decay curve. The linear slope of each decay curve yields T_{1c}. The T_{1c} values thus obtained for all the specimens are listed in Table 2.

As for the noncrystalline phase, the measurements were done by standard saturation recovery pulse sequence using diagram (b) in Fig. 2. The analysis was carried out for the magnitude of peaks appearing at around 31 ppm and associated with the chemical shift tensor of *n*-paraffin in liquid or polyethylene in solution [30]. This peak is strongly affected by the peak of orthorhombic crystal at signal of $\tau > 1.0$ s and the logarithm of ^{13}C magnetization vs. τ deviates from a linear relationship, but at $\tau > 0.5$ s the linear relationship could be obtained for all specimens. These results are summarized in Table 2.

To pursue more detailed analysis, the value of T_{2c} according to diagram (c) in Fig. 2. was obtained from the semilogarithmic plot of the peak heights of the line 31 ppm as a function of τ for the 25/75 component as shown in Fig. 10 as one of examples. The overall decay curve (a) can be clearly resolved into two parts, a rapid decay within 110 μs and a subsequent slow decay. The initial slope of the slower decay yield $T_{2c} = 2507$ μs which is recognized as the rubberlike amorphous component, while that with $T_{2c} = 103$ μs is much less mobile than the amorphous component. Therefore, as discussed by Horii et al. [25, 31] this component can be assigned to the interfacial noncrystalline component in construction of the lamellar structure. The results for all the components are listed in Table 3.

As illustrated in Tables 2 and 3, the T_{1c} values of crystallites of UHMWPE are almost independent of the composition within the experimental error. This tendency is similar to the fact that the composition is independent of

Table 2 The spin-lattice relaxation times of PE measured for the blend films unit (s^{-1})

Sample (PTFE/UHMWPE)	Crystalline components	Noncrystalline component
100/0		
75/25	12.1, 199.9, 972.4	0.368
50/50	9.57, 161.4, 1057.3	0.367
25/75	19.5, 190.5, 1194.2	0.324
0/100	13.6, 90.1, 410.4, 1064.9	0.376

Colloid & Polymer Science, Vol. 273, No. 7 (1995)

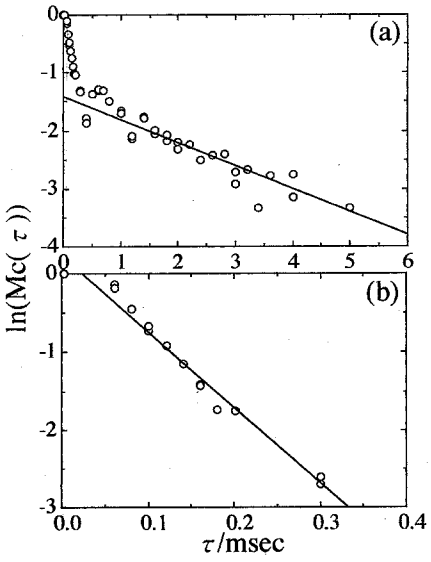

Fig. 10 Semilogarithmic plot as a function of τ measured for the blend film with the 25/75 composition to measure T_{2c}. (a) an overall decay curve and (b) a rapid decay curve

Table 3 The spin-spin relaxation times of PE measured for the blend films unit (μsec^{-1})

Sample (PTFE/UHMWPE)	Interfacial	Amorphous
100/0		
75/25	96.1	3724
50/50	96.2	3044
25/75	103	2507
0/100	72.6	2093

the crystal size in Table 1. Table 3 indicates that the composition independence of T_{1c} value of crystalline phase is in good agreement with the composition independence of crystallinity as shown in Fig. 3. On the other hand, the molecular mobility of the amorphous chain segments is postulated to be slightly active with increasing PTFE content, as the T_{2c} values increase with the content of PTFE. In contrast, the T_{2c} values associated with interfacial region are almost independent of the content of PTFE except UHMWPE homopolymer. Judging from the results in Tables 2 and 3, the content of UHMWPE is almost independent of the characteristics of crystallites and is rather sensitive to that of the amorphous region.

Conclusion

The blend films of PTFE and UHMWPE were prepared by kneading with the toque-rheometer at 320 °C, and their morphology and mechanical properties were investigated. The melting temperature of PTFE slightly decreased with increasing the content of UHWMWPE, while that of UHMWPE was almost independent of the blend content. The specimen with the 75/25 composition could be maintained at temperatures higher than 300 °C in spite of their incompatibility. This heat resistance effect is due to the fact that even in the temperature range higher than the melting temperature of UHMWPE, UHMWPE chains diffused within the PTFE fibrillar texture cannot be separated from the PTFE matrix. The crystallinity of PTFE decreased with increasing UHMWPE content. In contrast, the results obtained by ^{13}CNMR and x-ray diffraction indicated that the crystal size and the T_{1c} for crystal and noncrystalline components of UHMWPE were almost independent of the content of PTFE but T_{2c} for the amorphous region increased with the content.

Acknowledgement We are greatly indebted to Prof. Horii, Chemical Research Institute of Ktoyo University, for valuable discussion and suggestions for carrying out the NMR experiments. We also thank Dr. Kubo, Daikin Engineering Co. Ltd, for samples.

Appendix

The intensity distribution $I(x)$ from the test specimen is given by the convolution of the diffraction intensity distribution $G(x)$ of x-ray beam from an ideal pinhole slit and the broadening of diffraction intensity distribution $f(x)$ by the x-ray instrument used in this experiment. That is,

$$I(x) = \int_{-\infty}^{\infty} f(y)G(y-x)\,dy = G(x)f(x)\,. \qquad \text{(A-1)}$$

In Eq. (A-1), the function of $G(x)$ is represented by a Gaussian type,

$$G(x) = C\exp(-kx^2)\,, \qquad \text{(A-2)}$$

where C is a constant and k is given by

$$k = \pi/\beta\,, \qquad \text{(A-3)}$$

where β is the integral breadth of the diffraction peak. Since the distribution $f(x)$ can be determined by the profile of the diffraction peak of quartz, the optimum of k to obtain β can be determined by using a computer to give the best fit between experimental and calculated curves of $I(x)$ in Eq. (A-1).

References

1. Smith P, Lemstra PJ (1980) J Mater Sci 15:505
2. Smith P, Lemstra PJ, Pipper JPL, Kiel AM (1980) Collod Polym Sci 258:1070
3. Matsuo M, Inoue K, Abumiya N (1984) Sen-i-Gatsukaishi 36:696
4. Matsuo M, Sawatari C, Iida M, Yoneda M (1985) Polymer J 17:1197
5. Matsuo M, Sawatari C (1986) Macromolecules 19:2036
6. Furuhata K, Yokokawa T, Miyasaka K (1984) J Polym Sci Polym Phys Ed 22:133
7. Kanamoto T, Tsuruta A, Tanaka K, Porter RS (1983) Polymer J 15:327
8. Matsuo M, Sawatari C (1986) Macromolecules 19:2036
9. Mitsui H, Hoshi F, Kagiya T (1973) Polymer J 4:79
10. Hulse G, Kersting RJ, Wartul DR (1981) J Polm Sci Polym Chem Ed 19:655
11. Sawatari C, Matsuo M (1985) Colloid Polym Sci 263:783
12. deBoer J, van denBerg H-J, Pennings AJ (1985) Polymer 25:513
13. Matsuo M, Sawatari C (1986) Macromolecules 19:2028
14. Sawatari C, Matsuo M (1987) Macromolecules 20:1033
15. Sawatari C, Satoh S, Matsuo M (1990) Polymer 31:1456
16. Nagumanova EI, Mendiarov HG, Yokin VS (1973) Khim Khim Technol 16:1568
17. Nagarajan S, Stachurski ZH (1982) J Polym Sci Polym Phys Ed 20:989 ibid 20:1001
18. Torchia DA (1978) J Magn Reson 30:613
19. Quinn FA, Jr Madelkern L (1959) J Am Chem Soc 80:3178
20. Starkweather HW, Zoller P, Jones GA, Vega AJ (1982) J Polym Sci Polym Phys Ed 20:751, (1982) ibid 20:2159
21. Clark ES, Muss LT (1962) Zeitschrift fur Kristallographie Bd 117 S 119
22. Mababe S, Sakado A, Katada A, Takayanagi M (1970) J Macromol Sci Phys B 4:161
23. Suehiro S, Yamada T, Inagaki H, Kyu T, Nomura S, Kawai H (1979) J Polym Sci Polym Phys Ed 17:763
24. Bunn CW, Wowells (1954) Nature (London) 174:549
25. Nakagawa M, Horii F, Kitamaru R (1990) Polymer 31:323
26. Vander Hart DL (1979) Macromolecules 12:1232
27. Opella SJ, Waugh JS (1977) J Chem Phys 66:4919
28. Earl WL, VanderHart DL (1979) Macromolecules 12:762
29. Zhu Q, Horii F, Kitamaru R (1989) Nihon Reoroji Gakkaishi 17:35
30. Hama T, Suzuki T, Kosaka K (1975) Koubunshi–Ronbunshu 32:91
31. Kitamaru R, Horii F, Murayama K (1986) Macromolecules 19:636